Flux pinning in $YBa_2Cu_3O_{7-\delta}$ single crystals: Neutron irradiation and annealing

B. M. Vlcek, M. C. Frischherz, S. Fleshler, U. Welp, J. Z. Liu,* J. Downey,
K. G. Vandervoort, G. W. Crabtree, and M. A. Kirk
Materials Science Division, Argonne National Laboratory, Argonne, Illinois 60439

J. Giapintzakis
Material Research Laboratory, University of Illinois at Urbana–Champaign, Urbana, Illinois 61801

J. Farmer
Missouri University Research Reactor, Columbia, Missouri 65211
(Received 9 January 1992)

Results of dc magnetization on neutron (n) -irradiated $YBa_2Cu_3O_{7-\delta}$ single crystals are presented. The crystals were irradiated to a fluence of 2×10^{17} n/cm^2 ($E>0.1$ MeV). The magnetization has been measured at 10, 40, and 70 K for both field orientations. The magnetization is thereby obtained by cooling the sample in zero field to the desired temperature. Then the field is ramped in steps of 0.25 T up to 5 T and reversed in the same steps. At each field the magnetization is measured. The hysteresis ΔM is defined as the difference in magnetization between descending and ascending branches in the hysteresis loop. At 10 K, we observe an increase of the hysteresis by a factor of 3 for $\mathbf{H}\|c$ and by a factor of 10 for $\mathbf{H}\|a,b$ due to n irradiation. After irradiation, some of the crystals were annealed at 100, 200, and 300 °C for 8 h each. After each annealing step, the critical current densities and the transition temperatures were determined again. We observe that following the 300 °C annealing, the magnetization hysteresis for $\mathbf{H}\|a,b$ is almost reduced to the preirradiation level (a reduction in J_c of 90%), in contrast to the $\mathbf{H}\|c$ case, in which the decrease in hysteresis due to annealing is much less (a reduction in J_c of 30%). Crystals irradiated under the same conditions were used for transmission-electron-microscopy (TEM) studies. By comparison between TEM and magnetization measurements, the role of the cascade defects in pinning was determined. It is furthermore shown by TEM that the cascade defects do not anneal for comparable annealing temperatures. We find that the hysteresis for $\mathbf{H}\|c$ is governed by both the cascade defects which do not anneal and point defects or their clusters on the Y layers or CuO_2 planes which do anneal, whereas for $\mathbf{H}\|a,b$, pinning is determined by oxygen defects in the CuO chains which anneal due to oxygen diffusion.

INTRODUCTION

The effects of neutron irradiation on the properties of superconductors have become an active area of research during the past several years.[1–5] It has been observed that the irradiation-induced defects can act as effective pinning centers of magnetic-flux vortices and critical-current-density enhancements by factors of 3–10 have been reported in single crystals[1,5] and polycrystals[4] whereas smaller enhancements were observed in thin films.[2]

Since high-J_c values are of utmost importance for the practical use of the high-T_c cuprates, an identification of the pinning centers induced by neutron irradiation and their interaction with flux lines is of great interest. Much work has been done on the critical-current-density enhancements of one crystal as a function of increasing fluence.[5] The critical-current-density enhancement was found to saturate at fast neutron fluences near 1×10^{18} n/cm^2 ($E>0.1$ MeV).

Based on this work we chose a fluence at which the maximum critical current density is nearly reached. The defect density at this fluence is still low enough to avoid significant overlap between the defects.

Our paper focuses on the increase of the critical current densities of several single crystals at a fluence of 2×10^{17} n/cm^2 ($E>0.1$ MeV). The effect of the irradiation is determined by comparing the magnetization hysteresis of six single crystals for both directions of the applied field before and after irradiation.

Neutron irradiation produces atomic recoils with an energy spectrum ranging from the displacement threshold energy for the different sublattices (near 20 eV) to very high energies (> 100 keV). At the low-energy end of the spectrum point defects such as interstitials and vacancies are created. At the high recoil energies (> 30 keV) defect cascades are produced. A defect cascade is a small volume (~5 nm diameter), where due to the high-energy transferred, structural, disordering and possibly partial melting of the material occurs. This results in a severely damaged region. In metals these regions can collapse to dislocation loops,[6] and in semiconductors amorphous zones are observed.[7] The cascade defects are visible in conventional TEM studies, while point defects are not. In this study we show that both kinds of defects act as pinning centers.

Further insight into the contribution of the different defects to pinning can be obtained in annealing experi-

ments. Annealing has been done in two ways: room-temperature annealing and annealing at elevated temperatures. Three crystals were stored at about 30 °C for ten weeks after irradiation. After this time period, their hysteresis for $\mathbf{H}\|a,b$ and $\mathbf{H}\|c$ was measured again. One crystal was annealed at 100, 200, 300 °C for 8 h each after irradiation. After each annealing step, the hysteresis for $\mathbf{H}\|a,b$ and $\mathbf{H}\|c$ as well as the transition temperature were measured. We find that the effect of annealing on the magnetization hysteresis is much more pronounced for $\mathbf{H}\|a,b$ than for $\mathbf{H}\|c$, for both kinds of annealing.

Annealing experiments combined with TEM are a powerful tool to gain better understanding of the pinning mechanism in neutron-irradiated high-T_c compounds. Therefore, *in situ* TEM work was done after annealing temperatures and times comparable to the annealing schedule for the bulk material based on oxygen diffusion data.[8] The results show that at these temperatures the cascade defects produced by neutron irradiation do not disappear under annealing. Based on these results, we propose a model in which cascade defects are considered to be pinning centers for $\mathbf{H}\|c$ but are less significant for pinning for $\mathbf{H}\|a,b$.

The first part of this paper reports the results of the magnetization measurements for fields parallel to the c and a,b direction for all six crystals before and after irradiation. In the second part we show the effect of annealing on the magnetization and T_c measurements. The *in situ* annealing experiment using TEM will be discussed in the third part of this paper.

EXPERIMENTAL DETAILS

The samples were prepared by a self-flux method[9] and had typical sizes of $1\times1\times0.06$ mm^3. Six crystals were chosen and annealed in oxygen for 10 days at 450 °C prior to irradiation to ensure optimum oxygen content. The transition temperature T_c and transition width ΔT_c were measured in a home-built low-field superconducting quantum interference device (SQUID) magnetometer.[10] The samples were cooled in zero field and then measured during warming in an applied field of 1 Oe parallel to the c axis. The crystals have typical T_c values of 91–91.8 K and transition widths less than 0.4 K. Magnetization hysteresis measurements were taken in a quantum design SQUID magnetometer in fields up to 5 T at temperatures of 10, 40, and 70 K for both field orientations. Each measurement was carried out after cooling the sample in zero field from temperatures above T_c.

Because of the large anisotropy of $YBa_2Cu_3O_{7-\delta}$, magnetization measurements for fields applied along the a,b direction are very sensitive to a misalignment of the sample.[11] Since the crystals had to be remounted after irradiation and after each annealing step, the following precautions to achieve optimum orientation of the a,b plane with respect to the external field were taken: For the a,b measurements, the crystals were glued with their flat face to a quartz fiber, which is centered in the magnetometer by a weight. Furthermore, each time the sample was remounted the magnetization as a function of the applied field for $H<H_{c1}$ was measured. In the Meissner state (i.e., $H<H_{c1}$), the magnetic moment $\mathbf{M}$ is given by $\mathbf{M}=-\mathbf{H}/[4\pi(1-n)]$, where n denotes the demagnetization coefficient for the given field orientation and sample geometry. Therefore, a change of the orientation of the sample can be detected by a change in the slope of the $\mathbf{M}$ vs $\mathbf{H}$ curve for $H<H_{c1}$. For misorientation of the sample by an angle $\theta(\theta=0^\circ$ for $\mathbf{H}\|c)$ with respect to the applied field, the magnetization contains a component parallel (M_L) and a component perpendicular (M_T) to $\mathbf{H}$. M_L and M_T are given by[12]

$$M_L=-\frac{H}{4\pi}\left[\frac{\sin^2(\theta)}{1-n_\parallel}+\frac{\cos^2(\theta)}{1-n_\perp}\right], \tag{1a}$$

$$M_T=-\frac{H\sin(2\theta)}{8\pi}\left[\frac{1}{1-n_\parallel}-\frac{1}{1-n_\perp}\right], \tag{1b}$$

where $n_\parallel$ and $n_\perp$ are the demagnetization factors for the field orientations $\mathbf{H}\|a,b$ and $\mathbf{H}\|c$, respectively.

In our SQUID measurement only M_L can be determined. Thus a 3° difference in the angle would lead to a smaller slope by a factor of about 1.07 (with $4\pi n_\parallel=0.25$). This can easily be resolved in a SQUID measurement. By comparing the slopes in the Meissner state each time the samples were measured we were able to ensure that the orientation between the measurements did not change within 1°–2°. As additional check, the sample was simply remounted, and the hysteresis was remeasured under the same conditions. None of these procedures gave indication that misorientation is a problem in the results presented here.

The neutron irradiations were performed in the $H1$ position (outside the core but within the graphite reflector) of the University of Missouri Research Reactor (MURR) to a fluence of $(2\pm0.3)\times10^{17}$ n/cm^2 ($E>0.1$ MeV). For the TEM experiment discussed here, the sample was irradiated to a fluence of $(4\pm0.6)\times10^{17}$ n/cm^2 under the same conditions as the samples for the magnetization measurements. The higher fluence was chosen in order to achieve a higher visible defect density for the *in situ* annealing experiment. A detailed discussion of TEM investigations at different fluences will be presented in a forthcoming publication.

The neutrons have a mixed energy spectrum with a thermal peak, a $1/E$ epithermal regime and a fission peak. Dosimetry and spectrum determination were done using the foil activation method.[13] Thus, the neutron flux at full reactor power was determined [$(1.34\pm0.13)\times10^{13}$ n cm^{-2}s^{-1}, $E>0.1$ MeV], a fluence of 2×10^{17} n cm^{-2} corresponds therefore to an irradiation time of 4.1 h. Before irradiation the crystals were sealed in quartz tubes under He atmosphere. These tubes are contained in flooded aluminum cans and immersed in the reactor cooling water, which has a temperature of 43 °C during reactor operation.

Thinning of the neutron-irradiated crystals for TEM was done by crushing in methanol and transferal to a fine-mesh gold grid. Microscopy was performed in a PHILLIPS CM30 microscope operating at a comparatively low voltage of 100 kV in order to avoid electron-irradiation damage.[14] Dark-field (DF) images with an

operating Bragg reflection $g=(2,0,0)$ were taken. *In situ* heating experiments were performed by heating the sample to 200 °C and 400 °C for 10 min. Using the known diffusion coefficient for oxygen motion on the basal plane[8] the diffusion lengths in a,b for the microscope anneal are the same as for 8 h at 135 °C and 8 h at 250 °C, which roughly simulates the annealing experiments on the bulk crystals, at least for effects related to oxygen motion.

The magnetization hysteresis was measured one week after irradiation. Three crystals, Sample Nos. 1–3, were stored at temperatures slightly higher than room temperature for ten weeks and then measured again. One crystal, sample No. 6, was carefully cleaned and then annealed in air three weeks after irradiation at temperatures of 100 °C, 200 °C, and 300 °C for 8 h each. After each annealing step the crystal was characterized in terms of its hysteresis and critical temperature.

RESULTS

In order to compare the magnetization hysteresis of crystals with different mass and geometries, we convert ΔM to the critical current density using the anisotropic critical-state model of Bean.[15] This model treats the critical current density as field independent. The calculations for anisotropic critical current flow are done for a rectangular parallelepiped which resembles roughly the geometrie of the crystals used, neglecting however demagnetization effects. In Fig. 1 the components of the critical current densities for both field orientations and the corresponding dimensions of the crystal are shown. For fields applied along the a,b plane, $J_c^{ab}(\mathbf{H}\|a,b)$ denotes the component of the critical current along the

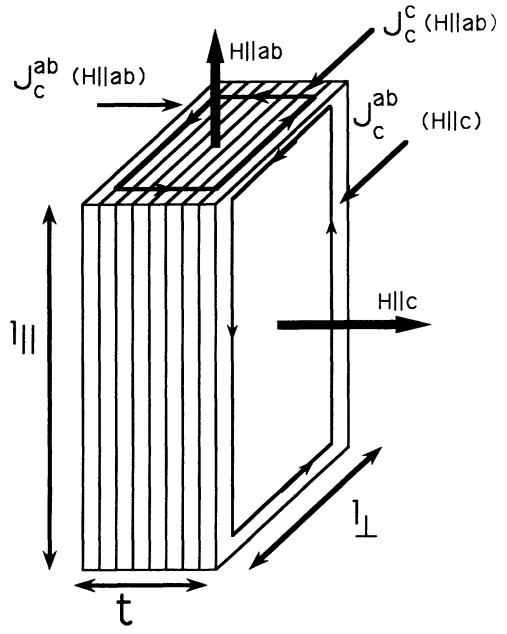

FIG. 1. A schematic picture of a platelet crystal displaying the three components of the critical current density for $\mathbf{H}\|a,b$ and $\mathbf{H}\|c$ is shown. The notation for the dimension of the crystals is included.

a,b plane and $J_c^c(\mathbf{H}\|a,b)$ is the critical current along the c direction. Similarly, J_C^{ab} $(\mathbf{H}\|c)$ is defined as the critical current flowing in the a,b plane when the field is applied along the c direction. For a platelet of thickness t, with length $l_\perp$ normal to the in-plane field direction and length $l_\parallel$ parallel to the in-plane field the relation between irreversible magnetization and critical current densities is given by [11,16]

$$\frac{20\,\Delta M_{ab}}{t}=J_c^{ab}(\mathbf{H}\|a,b)\left[1-\frac{tJ_c^{ab}(\mathbf{H}\|a,b)}{3l_\perp J_c^c(\mathbf{H}\|a,b)}\right], \quad \frac{tJ_c^{ab}(\mathbf{H}\|a,b)}{l_\perp J_c^c(\mathbf{H}\|a,b)}<1 \tag{2}$$

$$\frac{20\,\Delta M_{ab}}{t}=\frac{J_c^c(\mathbf{H}\|a,b)l_\perp}{t}\left[1-\frac{l_\perp J_c^c(\mathbf{H}\|a,b)}{3tJ_c^{ab}(\mathbf{H}\|a,b)}\right], \quad \frac{tJ_c^{ab}(\mathbf{H}\|a,b)}{l_\perp J_c^c(\mathbf{H}\|a,b)}>1 \tag{3}$$

$$\frac{20\,\Delta M_c}{l\perp}=J_c^{ab}(\mathbf{H}\|c)\left[1-\frac{l_\perp}{3l_\parallel}\right], \quad l_\perp<l_\parallel . \tag{4}$$

$\mathbf{H}\|c$

Figure 2 shows the critical current densities at three temperatures before (left column) and after irradiation (right column). The critical current density is calculated from the magnetization hysteresis using Eq. (4). Since the crystals are twinned, it is assumed that for $\mathbf{H}\|c$ the critical currents are isotropic in the a,b plane. The critical current densities at 10 K before irradiation are almost independent of the field above 1 T. The values are about 1.4×10^6 A/cm^2 at this field, with the exception of one crystal (No. 5) whose critical current density is lower ($\sim1\times10^6$ A/cm^2 at 1 T) and decreases with increasing field. All crystals show the same field dependence after irradiation at 10 K. Four crystals have similar J_c values [$(4-5)\times10^6$ A/cm^2] at fields above 1 T corresponding to an enhancement of J_c by a factor of 3 due to neutron irradiation. One crystal (No. 4) shows values twice as large.

The field dependence of the critical current density before irradiation at 40 K has nearly the same behavior for all crystals. Three crystals have about the same J_c values ($\sim2.5\times10^5$ A/cm^2 at 1 T), two of them, Nos. 4 and 5, have slightly lower J_c values ($\sim1.5\times10^5$ A/cm^2 at 1 T). After irradiation the same field dependence of the critical current densities is observed. Three crystals have similar J_c values of about 1.5×10^6 A/cm^2 at 1 T. This corresponds to an enhancement by a factor of about 10 due to irradiation with fast neutrons. Two crystals have higher values of J_c, the highest being 3×10^6 A/cm^2 at 1 T (Nos. 4 and 5), corresponding to an enhancement by a factor of 20.

An interesting behavior is found at 70 K. Before irradiation, we observe for three crystals again a field dependence for the critical current density with a pronounced maximum at 1 T and an irreversibility field of about 3 T. The other two crystals (Nos. 4 and 5) show reversible

magnetizations. After irradiation, we observe that crystals (Nos. 1–3), that showed a pronounced maximum in the dependence of their critical current densities on field and a irreversibility field before irradiation, exhibit J_c values of about 2.5×10^5 A/cm^2 at 1 T and about the same irreversibility field after irradiation. This corresponds to an enhancement of the critical current density by of a factor of 10. The two crystals which were reversible before irradiation (Nos. 4 and 5) show J_c values of about 9×10^5 A/cm^2 at 1 T and a field of irreversibility greater than 5 T. For these crystals, the enhancement factor would be infinite.

To summarize the results the following statements can be made. All crystals show enhancements of the critical current densities due to irradiation. For all crystals the post-irradiation critical current densities decrease monotonically with increasing field, even though the field dependences were different prior to irradiation. The factors by which the critical current densities are increased are larger at higher temperatures. Crystals with lower initial J_c values exhibit the highest critical current densities after irradiation. This trend becomes more pronounced with increasing measuring temperatures. It should be noted that the figures do not contain all the results of these six crystals: The enhancement of the critical current density of one crystal (No. 6) after irradiation was so huge that even at 5 T the field of full penetration was not reached at 10 K; the results of this crystal are therefore not included in Fig. 2.

$\mathbf{H}\|a,b$

For the crystals studied here, the condition $tJ_c^{ab}(\mathbf{H}\|a,b)/l_\perp J_c^c(\mathbf{H}\|a,b)>1$ is fulfilled, and Eq. (3) is applicable. In order to calculate this current density we assumed that the critical current density in the basal plane is the same for both directions of the applied field, $\mathbf{H}\|ab$ and $\mathbf{H}\|c$. This is not necessarily the case since the direction of the flux line and the direction of the Lorentz force acting on the flux line are different for the two field

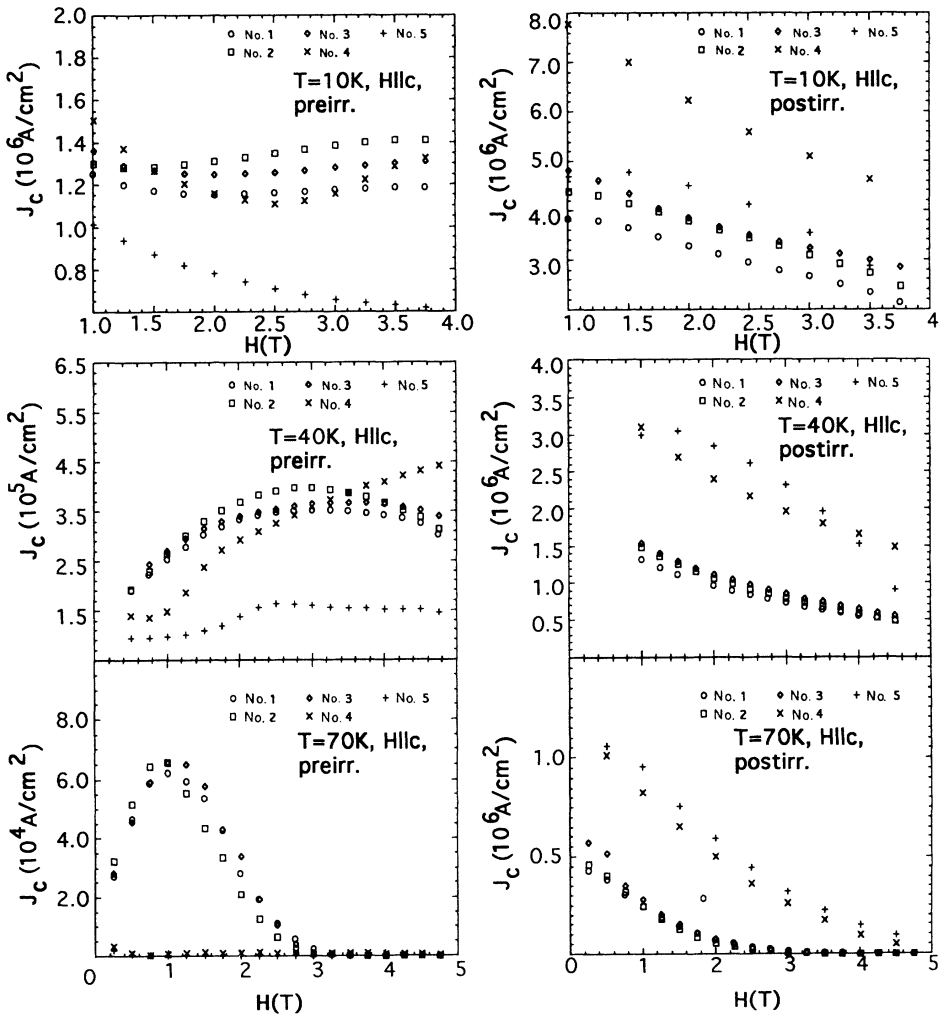

FIG. 2. Field dependence of the critical current density for $\mathbf{H}\|c$ of five crystals at 10 K (top), 40 K (middle) and 70 K (bottom) before irradiation (left column) and after irradiation (right column).

directions. It has been shown by Gyorgy[11] that these two current densities are about the same at 30 K. We furthermore applied an analysis based on the comparison of crystals with different aspect ratios[17] to distinguish between the three components of the critical current flow. This analysis shows that the above assumption is roughly correct at intermediate temperatures (40 K), whereas at lower or higher temperatures (10 and 70 K) a difference by about a factor of 2 has been found. However, the current flowing along the *ab* plane is always orders of magnitude larger than the current flowing along the *c* direction for $\mathbf{H}\|a,b$. Thus, the magnetization hysteresis is mainly determined by $J_c^c(\mathbf{H}\|a,b)$ and errors due to the assumption $J_c^{ab}(\mathbf{H}\|a,b)=J_c^{ab}(\mathbf{H}\|c)$ are negligible. Figure 3 shows the field dependence of critical current densities for $\mathbf{H}\|a,b$ before (left column) and after (right column) irradiation at 10 K, and 40 K assuming $J_c^{ab}(\mathbf{H}\|c)=J_c^{ab}(\mathbf{H}\|a,b)$.

The critical current densities before irradiation at 10 K show nearly the same field dependence. The values scatter from about 2×10^3 to 2×10^4 A/cm^2 at 1 T. After irradiation, the critical current densities do not exhibit the same field dependence. Four crystals show a decrease of the critical current density with increasing field, while two crystals (Nos. 1 and 2) show a maximum in their field dependence. The values for the critical current density at 1 T scatter between 4×10^4 and 8×10^4 A/cm^2. This corresponds to an increase by a maximum factor of about 10 due to irradiation.

At 40 K, we observe different field dependences of the critical current density before irradiation. Three crystals show a decrease of the critical current density with increasing field, the other three crystals (Nos. 1, 3, and 4) show a more Bean-model-like behavior. The values of the critical current density at 1 T range from 7×10^2 to 1.4×10^4 A/cm^2. After irradiation, we again observe different field dependences of the critical current density. Four crystals exhibit a decrease of the critical current density with increasing applied field, while two crystals show critical current densities independent of field after irradiation. The values range from 7×10^3 to 1.6×10^4 A/cm^2 at 1 T, which yields a maximum increase by a factor of 10. We do not show the 70-K data in this plot, since the values of the magnetization became too small to be measured accurately in this orientation of the field, especially before irradiation.

Summarizing the results, we observe an increase of the critical current density due to irradiation with fast neu-

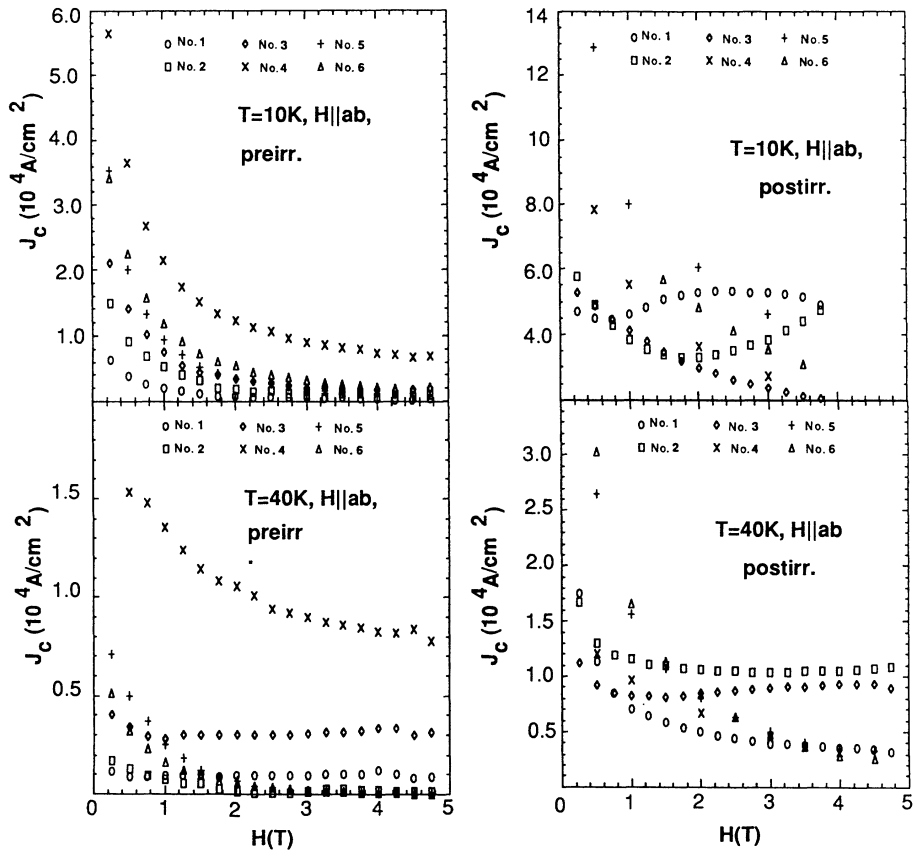

FIG. 3. Field dependence of the critical current density for $\mathbf{H}\|a,b$ of six crystals at 10 K (top), 40 K (middle), and 70 K (bottom) before irradiation (left column) and after irradiation (right column). The currents are calculated from Eqs. (3) and $J_c^{ab}(\mathbf{H}\|a,b)=J_c^{ab}(\mathbf{H}\|c)$.

trons. The values for the critical current densities show less scatter after irradiation than before irradiation; however, we do not observe any correlation between the critical current densities before and after irradiation for $\mathbf{H}\|a,b$.

ANNEALING

We studied two kinds of annealing: room-temperature annealing and annealing at elevated temperatures.

The results for room-temperature annealing (observed for crystals Nos. 1–3) for $\mathbf{H}\|a,b$ and $\mathbf{H}\|c$ are shown in Fig. 4. The hysteresis for $\mathbf{H}\|a,b$ is significantly reduced by room-temperature annealing, whereas the hysteresis for $\mathbf{H}\|c$ exhibits only a small decrease.

A similar behavior is found for annealing at elevated temperatures, shown in Fig. 5. Annealing at 100 °C has the highest impact on the critical current densities for fields applied along the a,b direction. Here a decrease of the hysteresis by about 50% is observed, whereas the magnetization hysteresis remains almost unchanged for $\mathbf{H}\|c$. Since the increase of the hysteresis for $\mathbf{H}\|c$ after irradiation of the crystal used for annealing at 100 °C, 200 °C and 300 °C (No. 6) was so huge that the field of full flux penetration H^*, was not exceeded, a calculation of the critical current density using Eqs. (3) and (4) is not thus reliable and therefore only the results of the hysteresis are presented here. Annealing at 200 °C and 300 °C leads to a decrease of the hysteresis for both directions of the applied field. The neutron irradiation induces a depression of T_c by ~ 0.5 K, which is fully recovered after the annealing (Fig. 6.)

TEM RESULTS

Figure 7(a) shows a micrograph of an area irradiated to 4×10^{17} n/cm^2 ($E>0.1$ MeV) with several defects (arrowed). Based on earlier TEM work on ion-irradiated $YBa_2Cu_3O_{7-\delta}$,[18] we conclude that these are defect cascades. Figure 7(b) shows the same area after the sample had been heated *in situ* to 200 °C for 10 min. All defects are still clearly visible. One small observable change is a small hint of two perpendicular sets of lines parallel to [110] and [110], respectively, (the tweed structure). As demonstrated in Fig. 7(c) the tweed structure fully develops after annealing for 10 min at 400 °C. Although the two biggest defects are visible after annealing, it is difficult to conclude whether the other defects are still present due to the background.

The tweed structure can be linked to the loss of oxygen in the microscope vacuum and, in fact, has been observed in oxygen-deficient crystals.[19] The diffusion length for

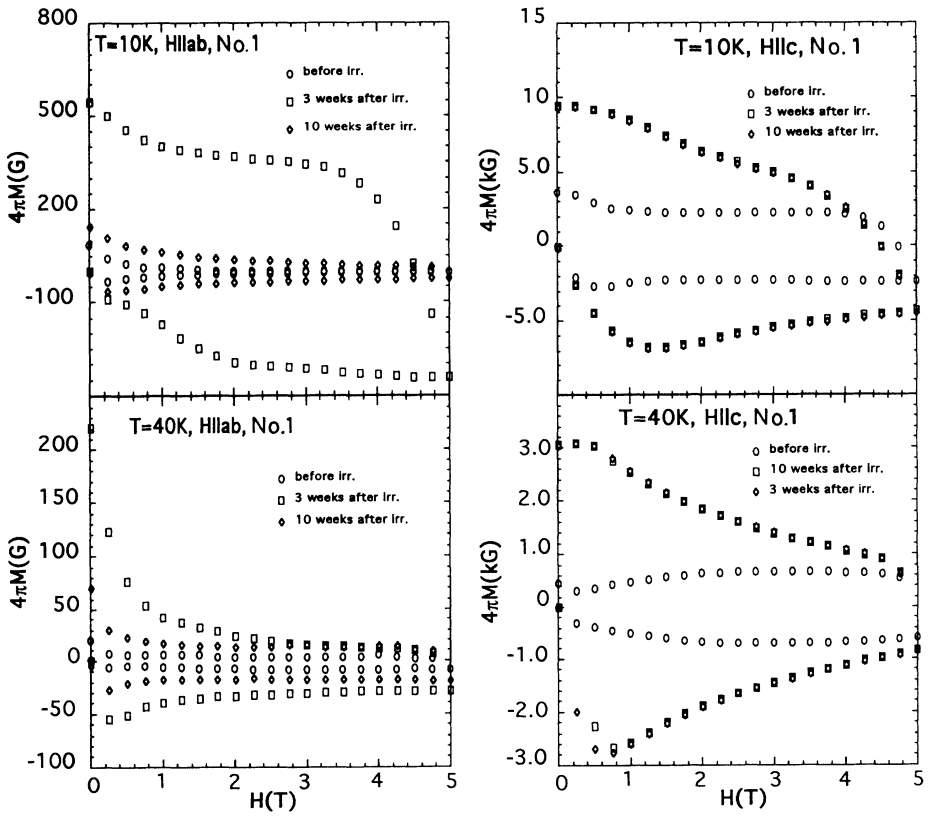

FIG. 4. Magnetization hysteresis as a function of the applied field before irradiation after irradiation and after storing the irradiated crystal at about 30 °C for ten weeks, for $\mathbf{H}\|a,b$ (left column) and $\mathbf{H}\|c$ (right column) at 10 K (top) and 40 K (bottom).

oxygen in the a,b plane is around 3 μm for 400 °C anneal, and around 3 nm $\|c$. Oxygen can leave the wedge-shaped edge ($\sim$100 nm thickness) of the sample by diffusion in the a,b plane.

In a forthcoming paper we will discuss experiments that show that defect cascades remain stable even after the samples have been stored at room temperature over long periods of time.

DISCUSSION

For $\mathbf{H}\|c$ we observe a correlation between preirradiation and postirradiation critical current densities in the sense that crystals with the initially lower J_c's exhibit the highest values after irradiation.

We use the following model to explain these results. The J_c's *before irradiation* are caused by an unknown defect structure which is more pronounced in the crystals which show pinning at 70 K (Nos. 1–3) than in those crystals which show reversible behavior at this temperature (Nos. 4 and 5). During irradiation, point defects as well as cascade defects are produced. The cascade defect density introduced by neutron irradiation is the same for all crystals. However, the density of small point-defect clusters can vary from crystal to crystal for the following reason. The point defects can migrate during irradiation and either cluster, recombine, or be trapped by already existing defects. Consequently, their density depends on the defect structure prior to irradiation. More specifically, crystals with initially low defect densities will be left with a higher amount of point defects or their clusters. These point-defect clusters act as additional effective pinning centers and are, together with the cascade defects, responsible for the higher critical current densities after irradiation. This explains why we observe higher critical current densities after irradiation for those crystals which exhibited the lowest critical current densities before irradiation (Nos. 4 and 5). Since we observe a stronger correlation between the critical current densities before and after irradiation at higher temperatures, we believe that these point defect clusters become more effective for pinning at higher temperatures.

The point defects or small clusters responsible for pinning for $\mathbf{H}\|c$ are most likely situated on the Y, Ba, or CuO_2 planes, since defects located on these layers lead to the greatest suppression of the order parameter. Electron-irradiation experiments identify Cu displacements on the CuO_2 layers as pinning centers for $\mathbf{H}\|c$.[20] The critical current density at 10 K and 1 T was found to increase by a factor of 2 after irradiation. This enhancement can be attributed to the introduction of point defects, since cascade defects are not produced by electron

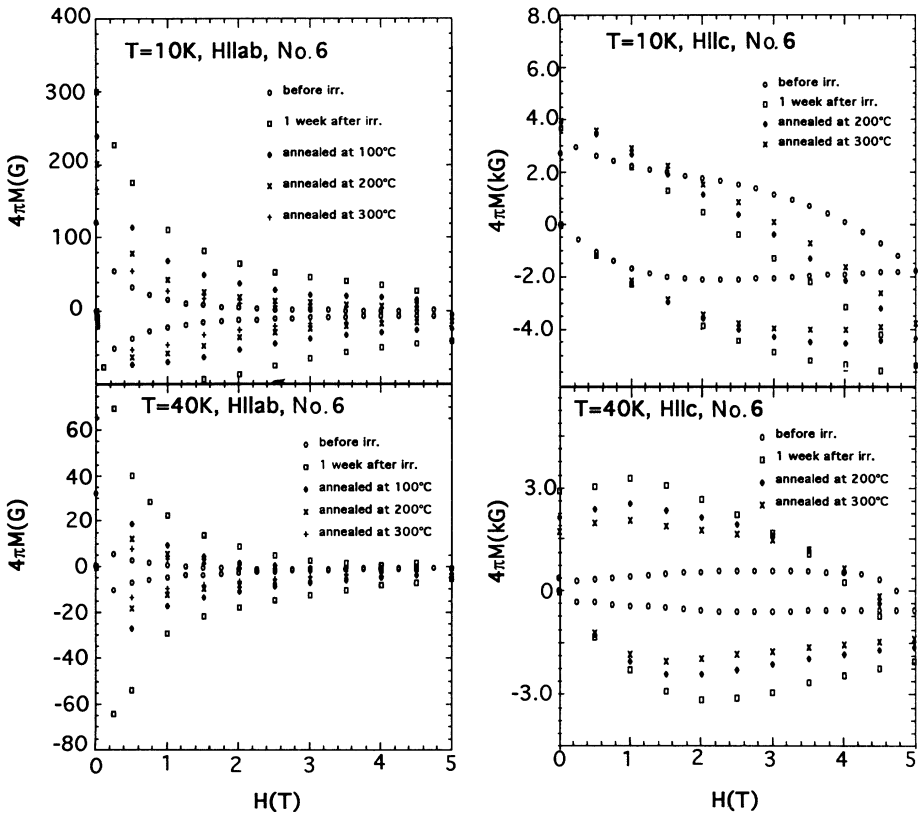

FIG. 5. Magnetization measurement as a function of applied field before irradiation, after irradiation, and after annealing the irradiated crystal at 100 °C, 200 °C, and 300 °C for 8 h each, for $\mathbf{H}\|a,b$ (left column) and for $\mathbf{H}\|c$ (right column) at 10 K (top) and 40 K (bottom).

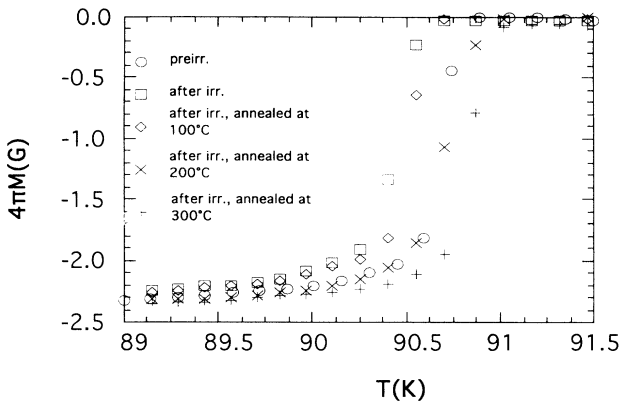

FIG. 6. T_c measurements of crystal No. 6, which was annealed after irradiation. The T_c value before irradiation was obtained in a different low-field SQUID than the other T_c values. The slightly higher-T_c value after the final annealing step at 300 °C can therefore be attributed to an absolute error in the temperature measurement caused by two different sensors.

irradiation. The same type of Cu displacements are present in the neutron-irradiated samples and lead to the effects discussed above.

Since the crystals before irradiation exhibit this second, broad maximum in their field dependence of the critical-current density[21] one might apply the granular model to explain the irradiation results. However, we show that this model cannot explain all the data presented here. Within the granular model, the observed increase with increasing field of the critical current densities at 40 and 70 K before irradiation is caused by small oxygen deficient regions with a lower T_c than the surrounding material. With increasing temperature and field, these regions become effective as pinning centers and lead to an increase of the critical current densities with increasing field. At higher fields, the crystal becomes fully granular and these oxygen-density deficient regions act as weak links; in this case, the critical current density would scale with the radius of the grains but not with the radius of the whole sample. In this picture, the vanishing hysteresis is attributed to a small or zero effective grain size, rather than to the disappearance of pinning within the grains. Thus, the crystals showing reversible behavior at 70 K (Nos. 4 and 5) are expected to be more granular than those crystals which show irreversible behavior at this temperature (i.e., Nos. 1–3).

Neutron irradiation would lead to an increase in pinning. However, the point of irreversibility would not increase since it depends on the effective grain size and is unaffected by neutron irradiation. This explains the results for the "less granular" samples. The "more granular" crystals show a considerable shift of the point of irreversibility and are not understood within this picture.

For fields applied along the a,b direction, the flux lines are centered on the chain planes. Defects on the CuO_2 or Y, Ba sublattices do not interact with the flux lines at low temperatures because of the small coherence length in the c direction. Pinning at temperatures where the coherence length exceeds the CuO_2 plane spacing (~ 80 K) is more complicated and not discussed here. Due to intrinsic pining,[22] the flux lines have only to be pinned for movements parallel to the CuO_2 plane. Pinning centers induced by neutron irradiation are therefore very effective for fields

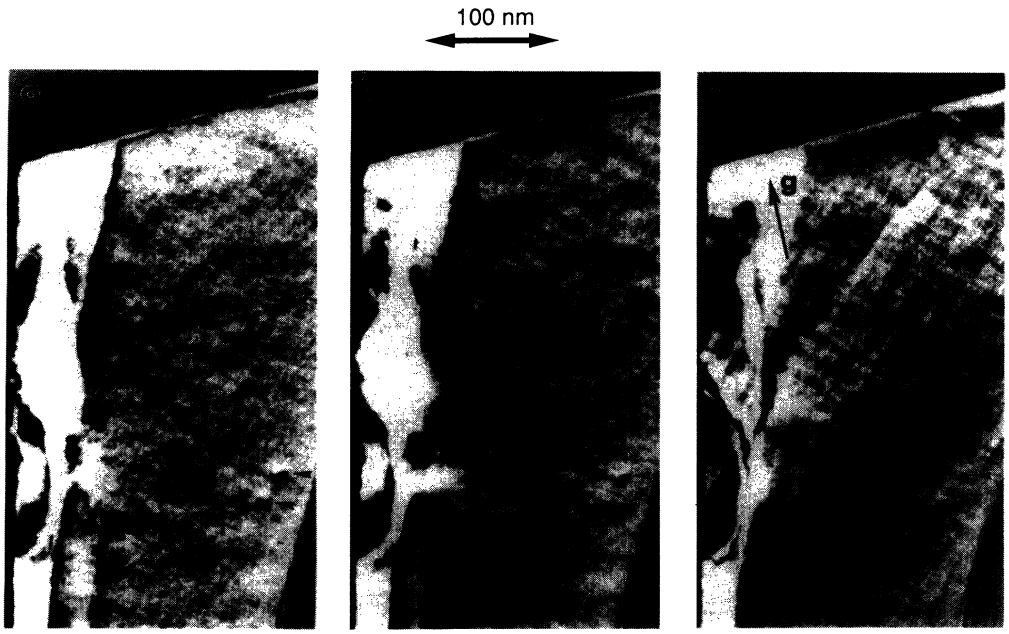

FIG. 7. (a) TEM micrograph of an area irradiated to 4×10^{17} n cm^{-2} showing some defect cascades (arrowed). The viewing direction is along [001]. (b) Same area as in (a) after *in situ* heating to 200 °C for 10 min, all defects from (a) are still visible. (c) Same area as in (a) after further heating to 400 °C for 10 min; the two largest defects are still visible; a network of lines parallel to [110] and [1$\bar{1}$0] [at 45° to $\mathbf{g}=(2,0,0)$] has developed.

in the a,b plane when the defects are situated on the CuO chain planes.

A surprising result for pinning for $\mathbf{H}\|a,b$ is obtained by our annealing experiments. We consider first the results of the room-temperature annealing measured for crystals Nos. 1–3. We observe that ten weeks after irradiation the hysteresis for $\mathbf{H}\|a,b$ is considerably decreased (50% at 10 K and almost by 100% at 40 K). Since the cascade defects remained, they do not seem to be very effective pinning centers for fields applied along the a,b plane. We suggest that pinning for $\mathbf{H}\|a,b$ is related to oxygen-deficient regions on the CuO chain plane, which may be produced during irradiation if the cation lattice in a cascade recrystallizes, with oxygen staying behind in the surrounding area. This idea is based on earlier work on ion-irradiated $YBa_2Cu_3O_{7-\delta}$,[18] where it is shown that $\sim 50\%$ of the defect cascades do not leave any visible defect behind. The defect cascade in these regions can be removed by annealing at room temperatures by oxygen diffusing back and in turn do not contribute significantly to pinning for $\mathbf{H}\|c$ as supported by a reduction of the hysteresis of less than 10%.

This is in agreement with annealing at elevated temperatures. Here we have to bear in mind that annealing at elevated temperatures not only leads to a recovery of oxygen-deficient regions on the basal plane but may also cause removal of the point defects or their clusters on the different sublattices. Their recovery causes, in contrast to the room-temperature annealing, a reduction of the hysteresis for $\mathbf{H}\|c$ as well (approximately 30%).

From Fig. 5 it can be seen that the hysteresis for $\mathbf{H}\|a,b$ is considerably decreased, after the final annealing step at 300 °C a reduction of the hysteresis by 90% is observed. Since we relate the recovery of the hysteresis for $\mathbf{H}\|a,b$ to annealing of oxygen-deficient regions on the basal plane, the recovery of T_c is explained in part by the same process. Further experiments to gain a better understanding of the decrease of the hysteresis as a function of annealing temperature for $\mathbf{H}\|a,b$ as well as $\mathbf{H}\|c$ are in progress. The recovery of T_c may also include a recombination of point defects in the CuO planes.

TEM measurements on annealing at room temperature and *in situ* TEM measurements on annealing at elevated temperatures do not show a reduction of the cascade defect density. The decrease in the hysteresis which we observe for annealing at elevated temperatures must therefore be caused by a reduction of the point defects or their small clusters.

CONCLUSIONS

After irradiating six crystals with fast neutrons, we observe an increase of the critical densities for $\mathbf{H}\|a,b$ and $\mathbf{H}\|c$ and also annealing effects which are different for these directions of the applied field. Low-dose neutron irradiation creates defect cascades and point defects, or more likely their clusters. These clusters may be higher in number for crystals with low defect densities prior to irradiation. Both types of defects (cascades and point defect clusters) act as pinning centers, the point-defect clusters being more effective for pinning at higher measuring temperatures. The cascade defects are not very effective pinning centers for fields applied along the a,b direction. The point defects and clusters created on or near CuO_2 planes are effective pinning centers for $\mathbf{H}\|c$ but not for $\mathbf{H}\|a,b$. Oxygen-deficient regions on the basal plane created by neutron irradiation act as the main pinning centers for $\mathbf{H}\|a,b$ and contribute little to pinning for $\mathbf{H}\|c$.

ACKNOWLEDGMENTS

We thank C. E. Jones for help with measurements on the low-field (SQUID). Furthermore, we also thank H. W. Weber, F. M. Sauerzopf, H. P. Wiesinger, and H. K. Vishwanathan for valuable discussions. This work was partly supported by the U. S. Department of Energy, Basic Energy Sciences-Materials Science under Contract No. W-31-109-ENG-38 (B. M. V, S. F., M. A. K., G. W. C., and J. D.) and the National Science Foundation-Office of Science and Technology Center for Superconductivity, under Contract No. STC8809854 (M. C. F. , U. W., J. G. and K. G. U.) and by the Midwest Superconductivity Consortium through DOE Grant No. DE-FG02-90ER45427 (J. F.).

*Present address: University of California at Davis.

[1]A. Umezawa, G. W. Crabtree, J. Z. Liu, H. W. Weber, W. K. Kwok, L. H. Nunez, T. J. Moran, and C. H. Sowers, Phys. Rev. B **36**, 7151 (1987).

[2]W. Schindler, B. Roas, G. Saemann-Ischenko, L. Schultz, and H. Gerstenberg, Physica C **169**, 117 (1990).

[3]H. Küpfer, I. Apfelstedt, W. Schauer, R. Flükiger, R. Meier-Hirmer, H. Wühl, and H. Scheurer, Z. Phys. B **69**, 167 (1987).

[4]J. R. Cost, J. O. Willis, J. D. Thompson, and D. E. Peterson, Phys. Rev. B **37**, 1563 (1988).

[5]F. M. Sauerzopf, H. P. Wiesinger, W. Kritscha, H. W. Weber, G. W. Crabtree, and J. Z. Liu, Phys. Rev. B **43**, 3091 (1991); for a review see H. W. Weber and G. W. Crabtree, in *Studies of High Temperature Superconductors,* edited by A. V. Narlikar (Nova Science, New York, in press), Vol. 9.

[6]W. Jäger, J. Microsc. Spectrosc. Electron. **6**, 437 (1981).

[7]J. S. Vetrano, M. W. Bench, I. M. Robertson, and M. A. Kirk, Met. Trans. A **20A**, 2673 (1989).

[8]S. J. Rothman, J. L. Routbort, U. Welp, and J. E. Baker, Phys. Rev. B **44**, 2326 (1991).

[9]D. L. Kaiser, F. Holtzberg, B. A. Scott, and T. R. McGuire, Appl. Phys. Lett. **51**, 1040 (1987).

[10]K. G. Vandervoort, G. Griffith, H. Claus, and G. W. Crabtree, Rev. Sci. Instrum. **62**, 2271 (1991).

[11]E. M. Gyorgy, R. B. van Dover, K. A. Jackson, L. F. Schneemeyer, and J. V. Waszczak, Appl. Phys. Lett. **55**, 283 (1989).

[12]S. Senoussi and C. Aguillon, Europhys. Lett. **12**, 273 (1990); S. Senoussi, S. Hadjoudj, R. Maury, and A. Fat, Physica C **165**, 364 (1990).

[13]L. Greenwood, J. Nucl. Mater. **21**, 108 (1982).

[14]M. A. Kirk, M. C. Baker, J. Z. Liu, D. J. Lam, and H. W.

Weber, in *High Temperature Superconductors,* edited by M. B. Brodsky, R. C. Dynes, K. Kitazawa, and H. L Tuller, MRS Symposia Proceedings No. 99 (Materials Research Society, Pittsburgh, 1988), p. 209.

[15]C. P. Bean, Phys. Rev. Lett. **8**, 250 (1962); Rev. Mod. Phys. **36**, 31 (1964).

[16]F. M. Sauerzopf, H. P. Wiesinger, and H. W. Weber, Cryogenics **30**, 650 (1990).

[17]P. C. Cronemeyer, T. R. McGuire, A. P. Malozemoff, F. Holtzberg, R. J. Gambino, L. W. Conner, and M. W. McElfresh, *Transport Properties of Superconductors,* edited by R. Nicolsky (World Scientific, Singapore, 1990), Vol. 25, p. 11.

[18]M. C. Frischherz, M. A. Kirk, J. Z. Liu, J. P. Zhang, and H. W. Weber, in *Proceedings of the 15th Radiation Effects Symposium of the American Society for Testing and Materials,* edited by R. E. Stoller, A. S. Kumar, and D. S. Gelles (American Society for Testing and Materials, Philadelphia, 1992), p. 733. M. C. Frischherz, M. A. Kirk, J. P. Zhang, J. Z. Liu, and H. W. Weber (unpublished).

[19]G. van Tendeloo and S. Amelinkx, J. Electron Microsc. Tech. **8**, 285 (1988).

[20]J. Giapintzakis, W. C. Lee, J. P. Rice, D. M. Ginsberg, I. M. Robertson, M. A. Kirk, and R. Wheeler, Phys. Rev. B (to be published).

[21]M. Daeumling, J. M. Seuntjens, and D. C. Larbalestier, Nature (London) **346**, 332 (1990).

[22]M. Tachiki and S. Takahashi, Solid State Commun. **70**, 291 (1989); **72**, 1083 (1989).

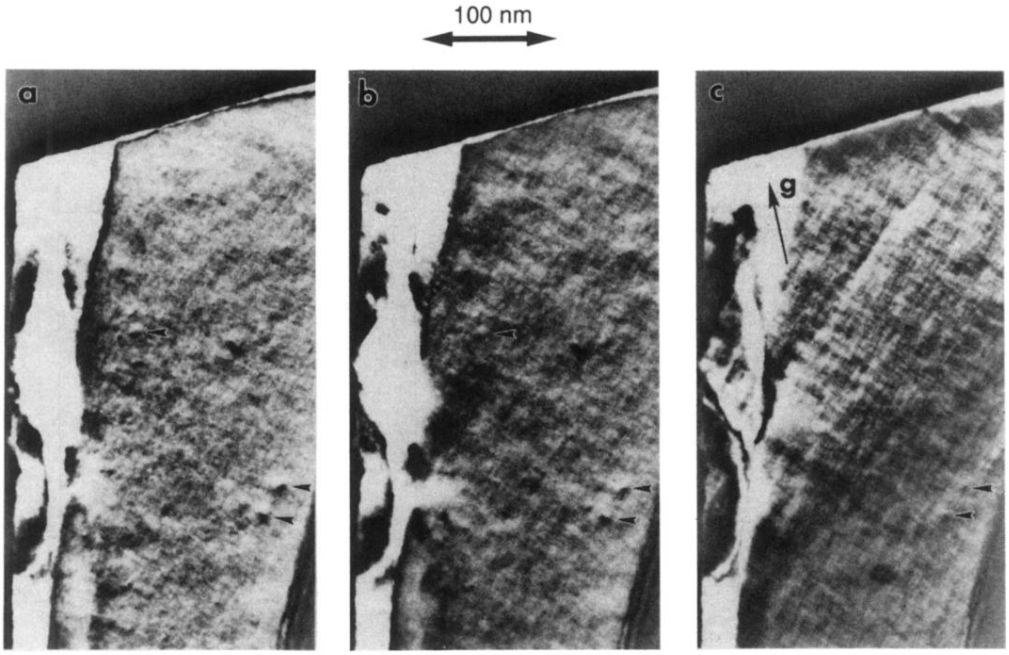

FIG. 7. (a) TEM micrograph of an area irradiated to 4×10^{17} n cm^{-2} showing some defect cascades (arrowed). The viewing direction is along [001]. (b) Same area as in (a) after *in situ* heating to 200 °C for 10 min, all defects from (a) are still visible. (c) Same area as in (a) after further heating to 400 °C for 10 min; the two largest defects are still visible; a network of lines parallel to [110] and [110] [at 45° to $\mathbf{g}=(2,0,0)$] has developed.